

Assessing the accuracy of forest above-ground biomass and carbon storage estimation by meta-analysis based close-range remote sensing

Jincheng Liu^{1,2*} , Zhuo Chen¹ and Ziyu Zhao³

¹ College of Natural Resources and Environment, Northwest A&F University, Yangling 712100, Shaanxi, China

² State Key Laboratory of Information Engineering in Surveying, Mapping and Remote Sensing, Wuhan University, Wuhan 430079, Hubei, China

³ Department of Resource Management, Tangshan Normal University, Tangshan 063000, Hebei, China

* Corresponding author, E-mail: jinchengl@nwfau.edu.cn

Abstract

The swift progress of close-range remote sensing necessitates a quantitative evaluation of its accuracy in estimating forest above-ground biomass (AGB) across diverse scales, forest types, methodologies, and variables. These evaluations will enhance the effectiveness of remote sensing in forest monitoring, reveal the carbon sequestration capability of forest vegetation, and underscore the critical function of forests as terrestrial carbon sinks. In this study, we designated R^2 as the effect size for the meta-analysis given that it is commonly regarded as a measure for estimating accuracy in AGB research, which indicates the explanatory capacity of independent variables. Utilizing 187 global investigations and 233 datasets, this research systematically assessed the accuracy (R^2) of ground light detection and ranging (LiDAR), unmanned aerial vehicles (UAVs), spectra, and red–green–blue (RGB) sensors across the single-tree, plot, and stand scales. The discrepancies in accuracy across the various research methods and the independent variables in the allometric growth equation were also assessed. The research indicated that ground lidar exhibited the best accuracy across all studies and was the most effective approach at both the single-tree and plot scales. Nonetheless, as the scale of the research broadened, both accuracy and sample size diminished. Furthermore, the variations from different approaches among different forest types were substantial; therefore, it was necessary to model these forest types explicitly. By integrating diameter at breast height (DBH or D) and tree height (H) as independent variables in the allometric growth equation, the method showed improved estimation accuracy. The estimation of AGB must address the issue of accumulated error arising from the interconversion of DBH and H, single-tree segmentation, and specific allometric growth equations, which are subsequently compounded at the plot and stand levels. Close-range remote sensing is currently the most efficient method for estimating forest AGB, surpassing conventional measurement techniques. Yet, due to sensor limitations, no single sensor achieved optimal results independently. The integration of multi-source data and scale adaptation strategies further enhanced the efficacy of close-range remote sensing, surpassing the conventional survey methods. Moving forward, efforts should prioritize cross-platform data standardization, deep learning model refinement, and the establishment of non-destructive validation systems to support high-precision forest carbon monitoring, in alignment with carbon management goals.

Citation: Liu J, Chen Z, Zhao Z. 2025. Assessing the accuracy of forest above-ground biomass and carbon storage estimation by meta-analysis based close-range remote sensing. *Forestry Research* 5: e017 <https://doi.org/10.48130/forres-0025-0017>

Introduction

Forests sequester atmospheric CO₂ in trees, understory vegetation, and soil through photosynthetic processes^[1–3], contributing approximately 76%–98% of the planet's terrestrial organic carbon pool^[4–6]. This vast carbon reservoir serves as a cornerstone in mitigating climate change and curbing the greenhouse effect^[7]. The development of high-resolution mapping of forest above-ground biomass (AGB), which underpins the assessment of forests' carbon sequestration capacity, has become integral to national climate strategies and the broader pursuit of green, low-carbon development. Accordingly, the scientific and precise estimation of forest AGB and carbon storage has emerged as a focal and extensively contested topic within the research community.

Forest AGB serves as an important indication for analyzing forests' community structure and ecosystem integrity^[8], as well as a key measure for evaluating the composition and quality of forest ecosystems^[9]. The assessment of forest AGB has evolved from traditional field-based inventories to remote sensing-driven methodologies^[10], leading to an integrated "satellite–airborne–terrestrial" research paradigm^[11]. In recent years, substantial advances in close-range remote sensing technologies^[12]—including unmanned aerial vehicles (UAVs), ground-based platforms, and

portable sensing instruments—have greatly increased their relevance in forest vegetation monitoring. Among them, UAV-based AGB estimation has emerged as a key method for assessing forest carbon sinks^[13,14]. This monitoring system allows for fine-scale delineation of near-ground structural features, effectively resolving the limits of classic standard-tree assessment techniques in heterogeneous stands with varying growth patterns and ages. Furthermore, it reduces observer-induced errors and labor intensity^[15], solidifying its position as a reliable and efficient tool for current AGB evaluation. Close-range remote sensing methods fall into four categories: red–green–blue (RGB)-based^[16], spectrum-based^[17], light detection and ranging (lidar)-based^[18–20], and radar-based^[21,22]. While these methodologies enable multi-scale observations ranging from single trees to entire plots and stands, a pronounced trade-off between spatial scale and estimation accuracy persists across different platforms. For example, ground lidar systems offer sub-centimeter precision in retrieving structural parameters at the single-tree level^[23,24], yet their accuracy tends to diminish when scaled up to plot-level analyses due to cumulative errors in single-tree segmentation. Conversely, UAV-based lidar excels in large-scale AGB assessments by delivering reliable estimates of tree height (H) and canopy structure, though it is constrained by limited canopy penetration and reduced efficacy in single-tree segmentation^[25–27]. Notably, AGB

estimation is also modulated by factors such as the species composition, stand structure, and forest age^[28]. Given that most natural forests comprise mixed-species assemblages rather than homogeneous monocultures, the application of species-specific AGB models and carbon conversion coefficients becomes imperative. Accordingly, there is a pressing need to examine the determinants of estimation accuracy across multiple spatial scales in tandem with prevailing research. These accuracy-related variables not only vary across observational scales but are also intricately linked to forest typologies, model inputs, and methodological frameworks—dimensions whose influence on AGB estimation remains insufficiently quantified.

Forest AGB estimation methods using close-range remote sensing can be broadly categorized into two methodological frameworks: The first integrates ground plot data with allometric equations^[29,30], while the second combines a limited number of ground plots with remote sensing data, which can be further subdivided into parametric and non-parametric approaches^[31,32]. These methodologies facilitate AGB estimation across multiple spatial scales, from single trees to plots, and ultimately to regional or landscape levels. The allometric approach, incorporating field-measured parameters into species-specific or region-specific equations, is widely regarded as the most accurate technique for single-tree AGB estimation. This method mitigates the challenges posed by labor-intensive and destructive sampling, while simultaneously enhancing the precision of AGB estimates at both the plot and stand scales^[33], thereby establishing itself as the prevailing strategy for forest AGB assessments^[34]. At the plot level, the integration of high-precision individual tree segmentation with localized allometric models further enables robust and spatially explicit AGB estimation. However, the scalability of this approach to broader regions is constrained by cumulative errors and model generalization limitations. To address these challenges, parametric and non-parametric methods leverage the outputs of allometric models as the ground truth to interpolate discrete tree-level measurements into continuous plot-scale AGB surfaces, thereby minimizing the fieldwork demands and enabling extrapolation to regional scales^[35–38]. Parametric models typically rely on statistically significant correlations between vegetation indices and AGB to construct predictive equations, allowing rapid estimates of AGB across large areas. In contrast, non-parametric approaches employ machine learning or deep learning algorithms in conjunction with close-range remote sensing data, effectively overcoming the limitations of parametric techniques, particularly under conditions involving high-dimensional variables or complex, non-linear relationships between the spectral features and AGB. These emerging methodologies offer promising avenues for future research, facilitating rapid, cost-effective, and non-destructive multi-scale estimates of forest AGB^[36,39,40].

Against the backdrop of global climate imperatives, achieving the twin goals of peak carbon peak and carbon neutrality (i.e., the carbon management goals in China) has become a pressing policy priority^[41], thereby underscoring the urgency of advancing methodologies for estimating forest carbon stocks and enabling the rapid, accurate assessment of forest carbon storage through close-range remote sensing^[42]. In this context, a comprehensive meta-analysis grounded in extensive empirical data is essential to elucidate the accuracy and reliability of close-range remote sensing techniques across varying spatial scales.

This study aims to address the following scientific questions: (1) How can we use meta-analyses to quantify the effects of scale, forest type, methodology, and independent variables on the accuracy of AGB estimations? (2) How can we enhance estimates of forest AGB through the integration of multi-source remote sensing data? (3)

What are the future directions for the development of close-range remote sensing monitoring systems?

Materials and methods

Literature search and screening

Relevant literature evaluating the stability of multi-scale forest AGB estimation based on close-range remote sensing was retrieved from the China National Knowledge Infrastructure database (www.cnki.net), the Wanfang Database (wanfangdata.com.cn), Google Scholar (<https://scholar.google.com>), VIP Database (<https://cqvip.com>), and Web of Science (www.webofscience.com). The search employed a set of keywords including 'optical remote sensing', 'UAV lidar', 'ground lidar', 'above-ground biomass', 'point cloud', 'multi-source remote sensing data', 'photogrammetry', and 'forest'. The literature retrieval period spanned from 1 January 2010 to 15 May 2025. In total, over 2,000 English-language publications and more than 400 Chinese-language studies were identified.

To ensure the accuracy and reliability of this study, the retrieved literature was screened in two stages on the basis of strict inclusion criteria. The initial screening involved reviewing the titles and abstracts to eliminate studies with irrelevant research areas, themes, methodologies, subjects, or data types. Duplicates and review articles were also excluded. Subsequently, a second round of screening was conducted according to the following criteria. First, studies had to be based on field experiments, excluding those conducted in greenhouse settings or involving potted plants. Second, eligible studies were required to report the standard deviation (SD), standard error (SE), and sample size (n) of the relevant variables, as well as the coefficient of determination (R^2) for the estimation results. Studies using alternative evaluation indices in place of R^2 were excluded. Mean values and standard deviations were obtained either directly from tables or extracted from figures using the Get Data Graph Digitizer software (<http://getdata-graph-digitizer.com>). Third, only studies focusing on AGB were included. Research involving belowground biomass, soil carbon storage, deadwood carbon, or litter carbon was excluded. Fourth, studies were limited to forest ecosystems, with those focused on grasslands, deserts, or other biomes excluded. Fifth, only literature utilizing close-range remote sensing platforms was retained, while studies relying solely on airborne or satellite remote sensing were excluded. Lastly, when extracting R^2 values, only the highest reported value for a given model was selected. In cases involving different spatial scales, tree species, or experimental sites, each was treated as an independent observation.

A total of 187 articles and 233 research data were collected, which were widely distributed and representative (Fig. 1). The database contained more than 1,000 variables, including the first author, year, sample size, SE, and other data (Supplementary Table S1).

Data calculation and processing

The present study adopted a single-group rate meta-analysis (Fig. 2) to quantitatively synthesize the R^2 reported in individual studies evaluating the accuracy of forest AGB estimations. Unlike traditional meta-analyses that compare effect sizes (ESs) between intervention and control groups, this approach consolidates single-group summary metrics (R^2) to generate a pooled estimate of the model's goodness-of-fit across heterogeneous experimental contexts. As R^2 is widely recognized as a robust indicator of estimation accuracy in AGB modeling, representing the proportion of variance in the dependent variable explained by the independent variables, it was designated as the ES for this analysis. In single-rate meta-analysis, accurate calculation of the standard error is critical for

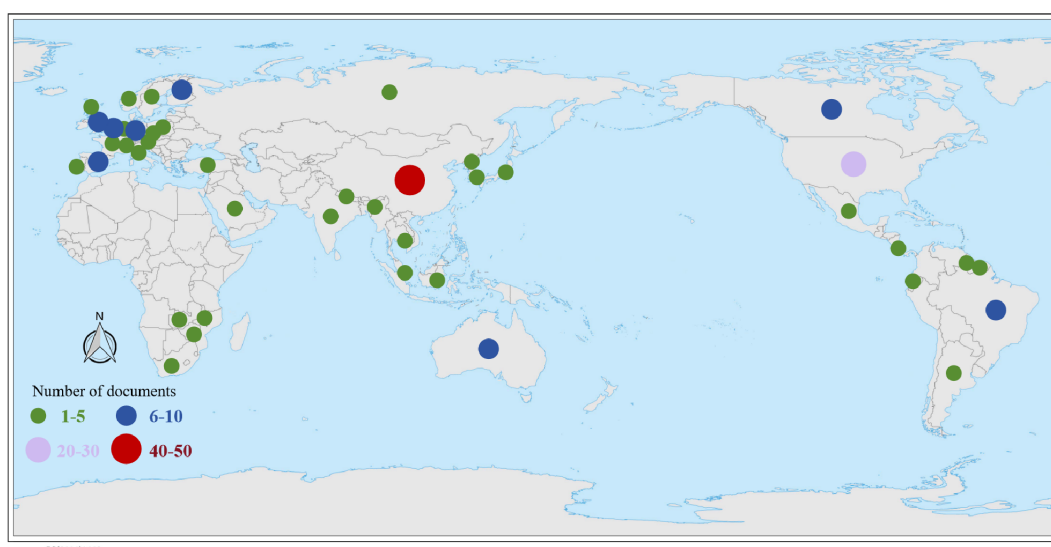


Fig. 1 Distribution of global literature.

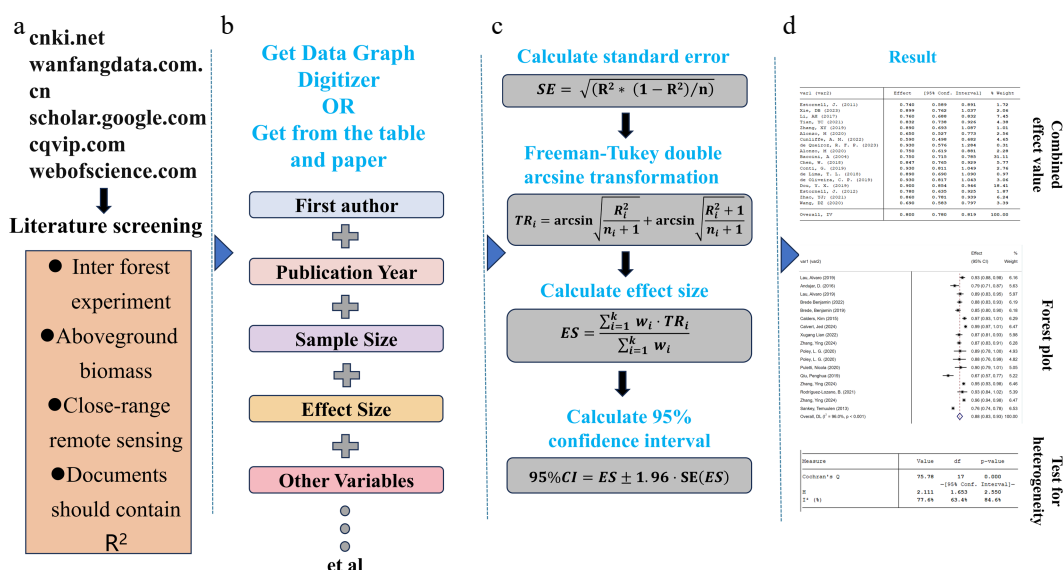


Fig. 2 Workflow of the meta-analysis. (a) Literature screening and search process; (b) extracting relevant data from the literature; (c) calculating the ES and 95% confidence interval (CI); (d) result.

capturing the uncertainty inherent in each study's ES. Accordingly, the standard error corresponding to each individual R^2 value was computed and employed to weight the relative contribution of each study in the overall aggregation. The standard error for single-group rates was calculated using the following formula Eq. (1):

$$SE_i = \sqrt{(R_i^2 \cdot (1 - R_i^2) / n_i)} \quad (1)$$

where, SE_i , R_i^2 , and n_i are the standard deviation, R^2 , and sample size of the i -th sample, respectively.

To overcome the inherent statistical limitation of variance being intrinsically linked to the mean, a variance-stabilizing transformation was applied prior to data synthesis. Specifically, the Freeman-Tukey double arcsine transformation Eq. (2) was utilized to normalize the distribution of R^2 values and to alleviate the effects of heteroscedasticity^[43] TR_i (transformed R_i) stabilizes the variance of coefficients of determination across studies through double arcsine transformation. This adjustment is critical for pooling accuracy estimates in random-effects meta-analysis.

$$TR_i = \arcsin \sqrt{\frac{R_i^2}{n_i + 1}} + \arcsin \sqrt{\frac{R_i^2 + 1}{n_i + 1}} \quad (2)$$

It is important to note that when the sample sizes are small and the ES values are close to 1, the confidence interval of the ES may exceed the theoretical bounds of [0, 1] following arcsine transformation. This phenomenon results from variance inflation during the inverse transformation process and represents a statistical artifact arising from the temporary expansion of the value domain in the course of meta-analytic aggregation, rather than a reflection of statistical unreliability. All such estimates were corrected using Freeman-Tukey adjustment to ensure conformity with the theoretical limits.

The pooled ES denotes the synthesized estimate of the overall rate, obtained by statistically integrating the findings from multiple independent studies. It serves as the most reliable approximation of the true probability of the target outcome within the broader population, while accounting for inter-study variability and heterogeneity. The 95% confidence interval (95% CI) is a critical indicator of the estimate's precision, signifying that there is a 95% likelihood that

the true ES resides within this interval. The transformed pooled ES was computed using the inverse variance weighting method Eq. (3), and the corresponding 95% CI was subsequently derived Eq. (4).

$$ES = \frac{\sum_{i=1}^k w_i \cdot TR_i}{\sum_{i=1}^k w_i} \quad (3)$$

$$95\%CI = ES \pm 1.96 \cdot SE(ES) \quad (4)$$

where Var represents variance, $w_i = \frac{1}{\text{Var}(TR_i)}$, and SE represents the standard error.

In the meta-analysis, heterogeneity among the included studies was evaluated using the χ^2 test and the I^2 statistic. The χ^2 test produces a p -value to assess the statistical significance of heterogeneity, while the I^2 statistic quantifies the proportion of total variation attributable to true heterogeneity rather than random error. A low p -value coupled with a high I^2 value indicates substantial heterogeneity across studies, whereas a high p -value and low I^2 value suggest relative homogeneity. To compute the p -value, Cochran's Q statistic was first calculated Eq. (5), which quantifies the dispersion in the accuracy of AGB estimation among studies. Under the null hypothesis of homogeneity, Q follows a χ^2 distribution with $k - 1$ degrees of freedom, where k represents the number of included studies. The χ^2 is generated by the software, and the p -value is determined by comparing Q with the corresponding χ^2 distribution Eq. (6). Subsequently, the I^2 statistic was derived to assess the magnitude of heterogeneity, based on the relationship between Q and its degrees of freedom Eq. (7).

$$Q = \sum_{i=1}^k w_i (ES_i - \overline{ES})^2 \quad (5)$$

$$P = P(\chi_{df}^2 > Q) \quad (6)$$

$$I^2 = [(Q - (k - 1)) / Q] \cdot 100\% \quad (7)$$

where ES_i is the ES of the i -th study, k is the number of studies, and df is the degree of freedom $df = k - 1$.

Values of $p \geq 0.10$ or $I^2 \leq 50\%$ indicated that there was no heterogeneity in the data and that the fixed effect model would be used for the combined analysis. Otherwise, $p \leq 0.10$ or $I^2 \geq 50\%$ indicated that there was statistical heterogeneity among the studies and that the random effect model then would be used for combined analysis. From the test results, only RGB at the stand scale and mixed forest, UAV lidar at the shrub scale, and ground lidar at the coniferous forest had poor heterogeneity, and the fixed effect model was used. All subgroups at other scales used the random effect model.

All relevant data were compiled and organized using Microsoft Excel 2021 (Microsoft, USA). The pooled ES and 95% CI values were computed using Stata 15SE (StataCorp LLC, USA), and forest plots were generated with PyCharm 2023 (JetBrains, Czech Republic).

Data packet

In this study, "close-range" remote sensing refers to non-contact measurement systems operating at altitudes less than or equal to 100 m above ground level. This classification included both ground-based and UAV-based platforms. To facilitate the analysis, sensors were categorized into three types according to their sensor modality: RGB sensors, spectrum sensors, and lidar sensors (Fig. 3). Lidar sensors were further classified according to the platform height into ground lidar and UAV lidar. Ground lidar encompassed terrestrial laser scanning (TLS), mobile laser scanning (MLS), backpack laser scanning (BLS), and hand-held lidar (HHL). In contrast, RGB and spectrum sensors were not classified by platform height; for example, UAV-based photogrammetry and ground-based photogrammetry were collectively categorized as RGB sensors. Currently, most methods for estimating AGB using radar rely on satellite data, with limited research utilizing UAV-based radar systems. Therefore, radar-based approaches were not included in the scope of this study. However, with the increasing availability and application of UAV-based radar technology, future studies are expected to integrate it into close-range remote sensing frameworks for AGB estimation.

This study further examined the impact of forest type on the accuracy of AGB estimation by classifying forests into four structural

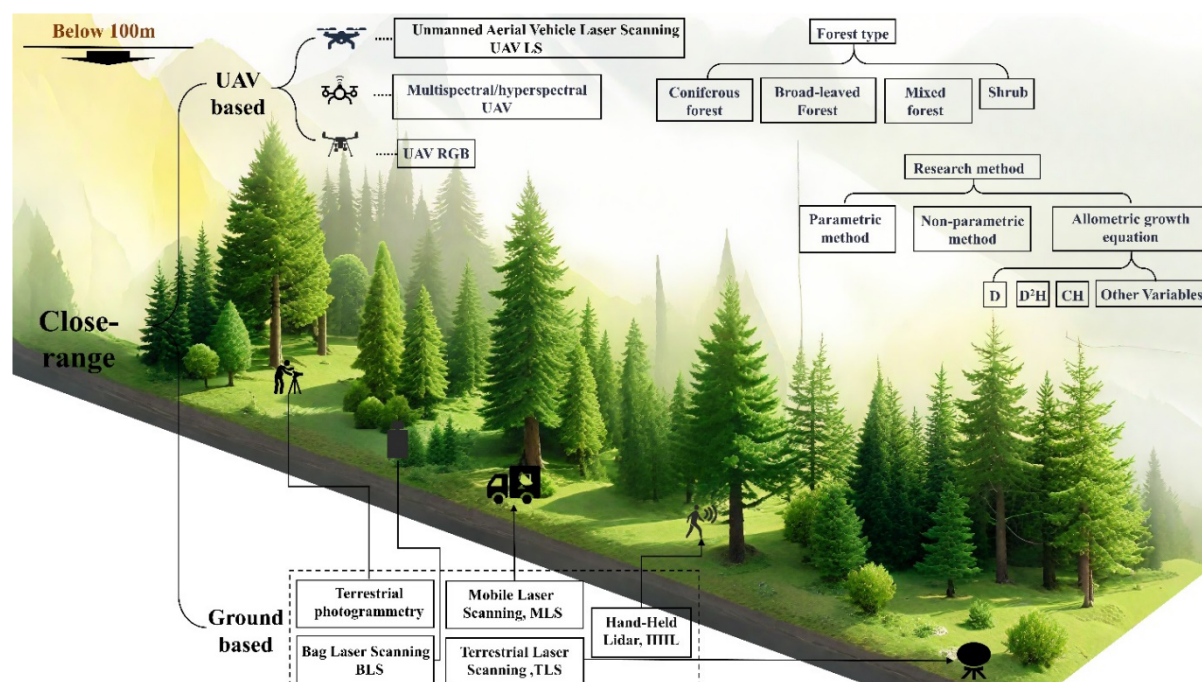


Fig. 3 AGB estimation systems using close-range remote sensing.

categories: coniferous forest, broadleaf forest, mixed forest, and shrubs. This classification framework enabled a systematic evaluation of close-range remote sensing performance across distinct vegetation structure. AGB estimation approaches were subsequently grouped into two primary categories: remote sensing synergy methods integrated with ground plots and allometric equations, and remote sensing synergy methods combined with a limited number of ground plots. The latter category was further subdivided into parametric and non-parametric models to assess their respective impacts on estimation accuracy.

Within the allometric growth equation framework, independent variables were classified according to combinations of diameter at breast height (DBH or D), crown width (CW), height (H), and other variables. The final classifications comprised D²H, H, D, and other variables (including unconventional combinations such as crown volume and crown density). This classification enabled a detailed analysis of how different independent variables affected estimation accuracy.

Results

Accuracy at different research scales

The meta-analysis revealed that the research scale significantly influenced the accuracy of close-range remote sensing techniques (Fig. 4). At the single-tree scale (which accounted for 56.55% of the sample size, Table 1), ground lidar exhibited the highest pooled ES (ES = 0.93; 95% CI: 0.92–0.95), significantly outperforming UAV lidar (ES = 0.81; 95% CI: 0.78–0.84) and RGB (ES = 0.8; 95% CI: 0.71–0.88).

This discrepancy arose from the subcentimeter point cloud resolution of ground lidar^[23], which allowed the direct extraction of DBH and H, facilitating high-precision fitting of the D²H allometric growth equation. In contrast, UAV lidar and RGB were constrained by limited canopy penetration, which led to missing subcanopy structures and higher segmentation errors, prevented direct acquisition of single-tree diameter parameters, and ultimately reduced the accuracy of estimation at this scale.

At the plot scale (which accounted for 32.98% of the sample size), the ground lidar also achieved the highest pooled ES (ES = 0.87; 95% CI: 0.81–0.93), suggesting its reliability in AGB estimation at this scale. However, UAV lidar exhibited an unexpectedly low ES (ES = 0.76; 95% CI: 0.61–0.84) compared with its theoretical capacity for rapid large-scale acquisition, attributed to point cloud sparsity and computational limitations in data processing^[44].

At the stand scale (which accounted for 10.48% of the sample size), all methods except spectra (ES = 0.74; 95% CI: 0.66–0.83) achieved high ES, which was sufficient to prove their reliability at this scale. Although the ground lidar had the highest ES on all three scales, the increase in the research scale reduced the sample size and the accuracy, so the workload and uncertainty were significantly improved^[45]. Therefore, the use of UAV RGB, especially UAV lidar, should be the preferred method at the stand scale^[46].

Accuracy in different forest types

There were significant differences in technical performance among different forest types (Fig. 5). Ground lidar had the highest ES in all forest types. In addition, the spectra (ES = 0.84; 95% CI: 0.75–0.92) had the highest ES in broadleaf forests (which accounted

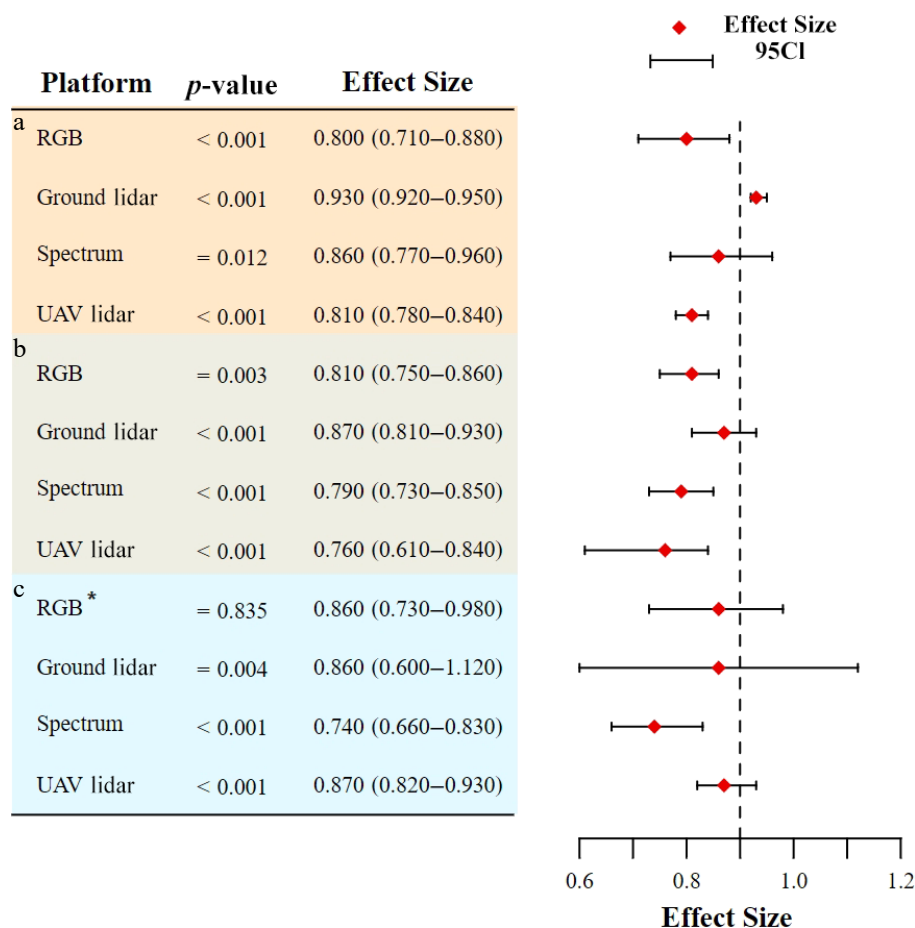


Fig. 4 Effects of different research scales on forest AGB estimation: (a) Single-tree scale; (b) plot scale; (c) stand scale. * indicates that a fixed effects model was used.

Table 1. Statistical table of sample size at different research scales.

| Scale of study | Sensor type | Number of samples | Sample proportion (%) | r^2 (%) |
|----------------|--------------|-------------------|-----------------------|-----------|
| Tree | UAV lidar | 38 | 19.90 | 97.6 |
| | Ground lidar | 42 | 21.99 | 75.8 |
| | RGB | 24 | 12.57 | 95.8 |
| | Spectra | 4 | 2.09 | 72.7 |
| Plot | UAV lidar | 31 | 16.23 | 97.0 |
| | Ground lidar | 7 | 3.66 | 73.5 |
| | RGB | 13 | 6.81 | 59.5 |
| | Spectra | 12 | 6.28 | 68.3 |
| Stand | UAV lidar | 13 | 6.81 | 86.6 |
| | Ground lidar | 2 | 1.05 | 88.3 |
| | RGB | 3 | 1.57 | 0.0 |
| | Spectra | 2 | 1.05 | 90.8 |
| Total | | 191 | 100 | |

for 20.43% of the sample size, Table 2). In coniferous forests, RGB had higher accuracy (ES = 0.81; 95% CI: 0.73–0.89) than the other three sensor types. It may be that the texture features of RGB images were easier to extract due to the single-canopy structure. In the mixed forest, the spectra (ES = 0.66; 95% CI: 0.25–1.07) were limited by the signal saturation of dense canopy. The accuracy of AGB estimation in shrubs was generally low (RGB ES = 0.85; 95% CI: 0.75–0.95; ground lidar ES = 0.83; 95% CI: 0.75–0.91). Because the vertical structure of low vegetation was difficult to capture by lidar, it was necessary to combine high-resolution ground RGB images to extract the data on plant density^[47].

Accuracy with different research methods

The results showed that (Table 3, Fig. 6a) there was no significant difference in accuracy among the three methods ($p < 0.001$). As the standard method of traditional AGB estimation, the allometric growth equation obtained the highest combined ES (ES = 0.83; 95% CI: 0.81–0.86). The non-parametric method (ES = 0.82; 95% CI: 0.80–0.85) also achieved good performance which was basically the same as that of the allometric growth equation (Δ ES = 0.01), probably due to the complex non-linear relationship between remote sensing features and AGB that machine learning algorithms can capture. In addition, the non-parametric method had high flexibility and was more adaptable to forests with multiple species and complex structures^[48]. In contrast, the parametric method showed lower accuracy (ES = 0.80; 95% CI: 0.76–0.85), which might be limited by the problem of signal saturation in dense canopies where the vegetation index was insensitive.

Accuracy with different independent variables

The results (Table 4; Fig. 6b) showed that D²H (ES = 0.90; 95% CI: 0.88–0.93) and D (ES = 0.91; 95% CI: 0.85–0.97) had the highest ES. Therefore, the allometric growth equation with D as the independent variable had high accuracy in estimating AGB. D is a commonly used variable in forest surveys. Due to their mature measurement methods and high accuracy, they provide reliable basic data for AGB estimations. In contrast, models with only H as an independent variable had the lowest effect (ES = 0.72; 95% CI: 0.56–0.89). This difference might arise from inaccuracies in measuring H and the fact that H may not adequately reflect trees' morphological characteristics

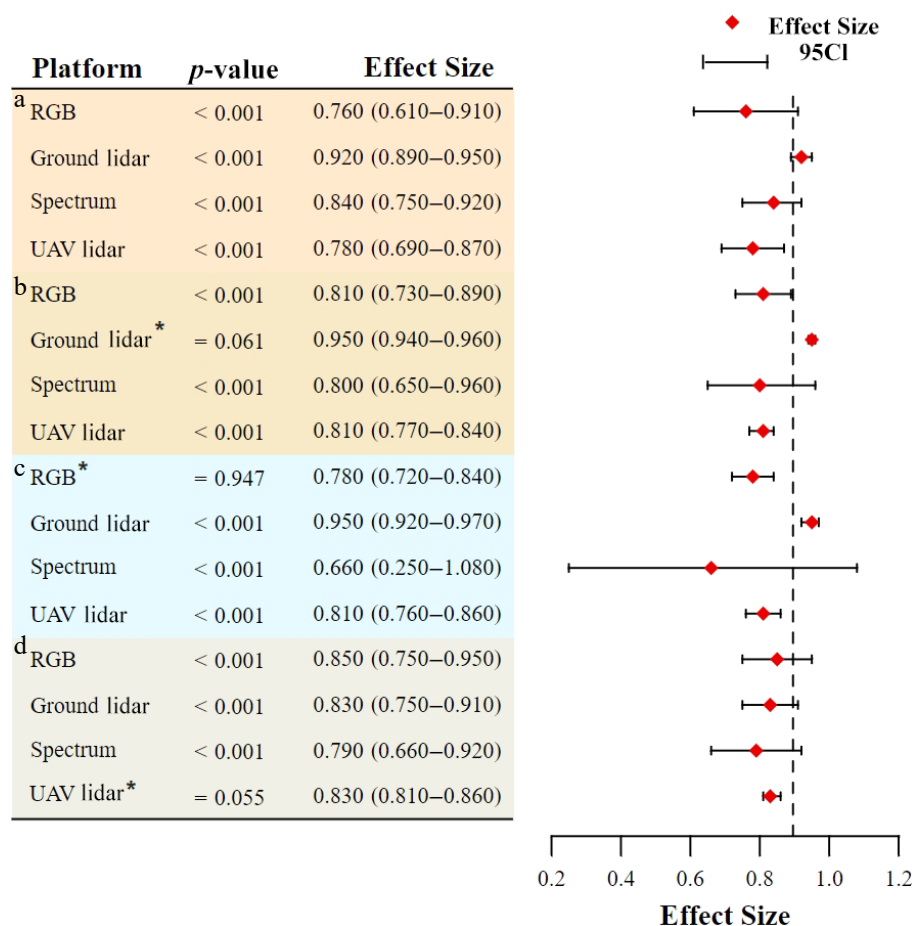


Fig. 5 Effects of different forest types on forest AGB estimations: (a) broadleaf forests; (b) coniferous forests; (c) mixed forests; (d) shrubs. * indicates that a fixed effects model was used.

Table 2. Statistical table of samples in different forest types.

| Type of forest | Sensor type | Number of samples | Sample proportion (%) | r^2 (%) |
|--------------------|--------------|-------------------|-----------------------|-----------|
| Broadleaf forests | UAV lidar | 22 | 11.52 | 98.2 |
| | Ground lidar | 14 | 7.33 | 42.1 |
| | RGB | 11 | 5.76 | 97.7 |
| | Spectra | 6 | 3.14 | 83.3 |
| Coniferous forests | UAV lidar | 20 | 10.47 | 85.8 |
| | Ground lidar | 12 | 6.28 | 42.1 |
| | RGB | 11 | 5.76 | 77.4 |
| | Spectra | 4 | 2.09 | 83.3 |
| Mixed forests | UAV lidar | 31 | 16.23 | 97.7 |
| | Ground lidar | 17 | 8.90 | 80.9 |
| | RGB | 6 | 3.14 | 0.0 |
| | Spectra | 3 | 1.57 | 99.6 |
| Shrubs | UAV lidar | 9 | 4.71 | 47.4 |
| | Ground lidar | 8 | 4.19 | 80.6 |
| | RGB | 12 | 6.28 | 88.8 |
| | Spectra | 5 | 2.62 | 86.0 |
| Total | | 191 | 100 | |

Table 3. Statistical table of samples with different research methods.

| Research method | Number of samples | Sample proportion (%) | r^2 |
|----------------------------|-------------------|-----------------------|-------|
| Parametric method | 95 | 40.77 | 98.6 |
| Non-parametric method | 62 | 26.61 | 91.9 |
| Allometric growth equation | 76 | 32.62 | 97.2 |
| Total | 233 | 100 | |

nor fully capture all factors influencing AGB^[29]. Conversely, other variables ($ES = 0.79$; 95% CI: 0.72–0.87), such as those derived from crown height equations or equations using crown volume and crown density as predictors, offer advantages. These independent variables are readily obtainable, as they can be directly retrieved from UAV lidar data. This facilitates large-scale rapid estimation and mapping of AGB, capabilities that are often lacking when using traditional allometric equations.

Multi-source vs. single-sensor accuracy

Multi-source data collaboration has been a hot spot in AGB estimation over recent years, as well as in close-range remote sensing research. Therefore, this study compared the accuracy of multi-source close-range remote sensing data with that of single-sensor remote sensing data (Fig. 6c). Looking at the results alone, it appeared that multi-source data ($ES = 0.8$; 95% CI: 0.77–0.84, Table 5) did not significantly improve the estimation accuracy of AGB compared with single data sources and were even lower than the ES of ground lidar ($ES = 0.93$; 95% CI: 0.92–0.94). However, from the perspective of specific research contexts, two key factors contributed to this outcome. First, substantial heterogeneity existed across forest plots. Multi-source remote sensing was typically applied to forests characterized by complex vertical stratification and dense horizontal structures—environments that were often inaccessible to manual survey efforts. In such cases, relying on a single data source, particularly ground lidar, was unlikely to yield comparable accuracy^[49]. Second, differences in the research scale played a critical role. Ground lidar was predominantly employed at the single-tree and plot scales, whereas multi-source remote sensing was more frequently utilized for large-scale AGB estimation^[34]. At such broader scales, the accuracy of estimation tended to decline, and the inherent complexity of forest structure further exacerbated this reduction in precision^[50,51]. Therefore, the coordinated integration of multi-source data emerged as a robust

and effective strategy, enabling compensation for the limitations of individual data types and facilitating more accurate estimations of AGB under structurally complex stand conditions.

Discussion

Accuracy at single-tree scale

The meta-analysis revealed that the research scale played a decisive role in shaping the estimation accuracy of close-range remote sensing technologies. At the single-tree scale, ground lidar exhibited significantly higher ES than UAV lidar, underscoring its superior performance in this context. This advantage stemmed from the capabilities of both TLS and mobile laser scanning (MLS), which excelled in capturing the three-dimensional structural attributes of individual trees with high precision^[23,52–54]. These systems demonstrated remarkable accuracy in estimating total biomass, stem biomass, and branch biomass, and numerous studies have confirmed that ground lidar has reached a mature level of application for single-tree AGB estimation, with predictive accuracy approaching unity. In contrast, UAV lidar-based estimation at the single-tree scale typically relied on generating a canopy height model (CHM) by subtracting a digital elevation model (DEM) from a digital surface model (DSM) derived from point cloud data^[24]. This process requires extensive supplementary spatial information, such as ground control points and high-resolution digital terrain models^[32]. Alternatively, single-tree segmentation algorithms were employed to extract structural parameters, such as DBH, H , and C , which were then incorporated into allometric equations for estimating AGB^[29,55]. As a result, the precision of DBH and H extraction has become critical to the reliability of estimation. However, UAV lidar faces inherent limitations at low operating altitudes, including canopy occlusion and laser pulse attenuation or scattering, which hinder effective penetration into subcanopy layers^[56]. This constraint significantly compromised the acquisition of key understory information, thereby reducing the accuracy of single-tree AGB estimates. In recent years, to address these limitations, researchers have sought to capitalize on UAV lidar's strengths in capturing canopy-level metrics such as H and CW ^[30,57,58]. These features could be used to infer DBH^[19] or to apply allometric models that do not require DBH as an input, offering alternative pathways for accurate AGB estimation in structurally complex forest environments.

Furthermore, the H and CW parameters extracted from UAV lidar could be effectively integrated with DBH measurements derived from ground lidar to enhance the accuracy of AGB estimation^[25,59]. In addition, several studies have demonstrated that the fusion of UAV lidar with hyperspectral imagery markedly improved the explanatory power of AGB estimation models^[60], thereby enabling high-resolution mapping of forest AGB^[48,61]. These findings collectively indicated that for high-precision AGB estimation at the single-tree scale, ground lidar should be regarded as the preferred method. Nevertheless, its application remains constrained by substantial time investment and limited spatial coverage, presenting practical challenges for large-area implementation.

Accuracy at plot and stand scales

When the scale was extended to the plot scale, the ground lidar and RGB methods showed high accuracy. Ground lidar is unable to measure areas that are difficult to reach, whereas UAV-based lidar is beneficial for conducting high-resolution tree canopy mapping in steep mountainous areas. It complements traditional methods and has thus been widely used for estimating forest AGB. Nevertheless, the measurement accuracy of UAV lidar at the small plot scale has not yet been widely recognized, as the point cloud data are

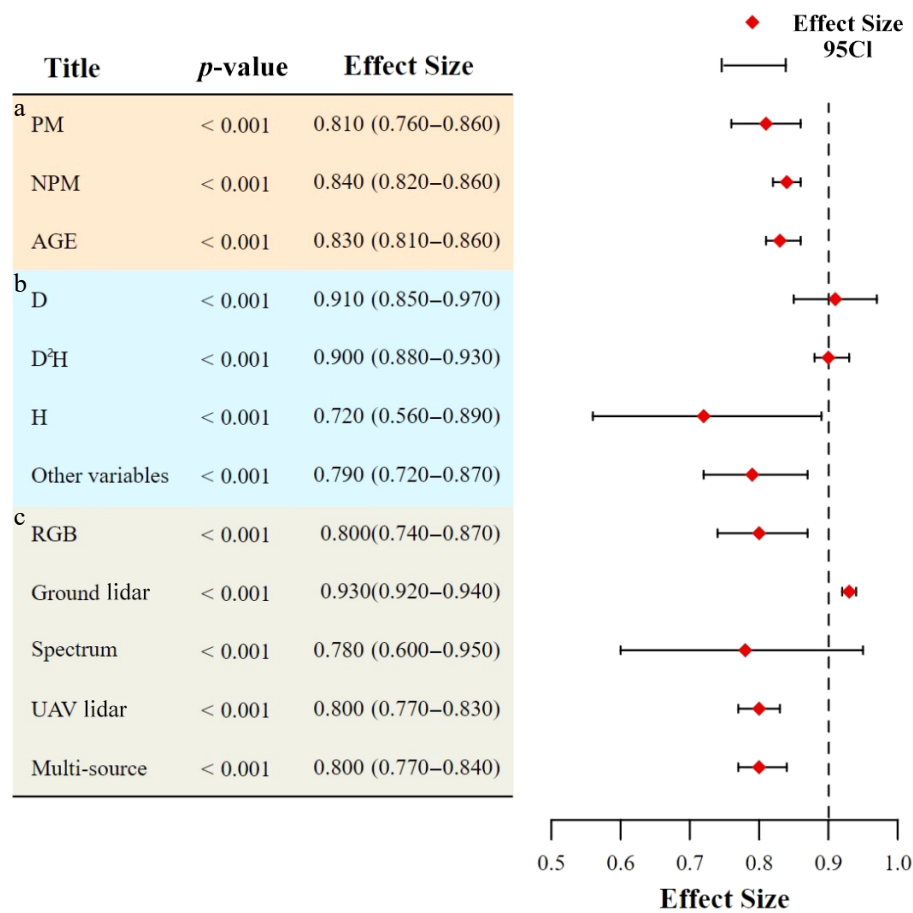


Fig. 6 AGB estimation accuracy of different research methods, different independent variables, and different platforms. (a) Different research methods. PM, parametric method; NPM, non-parametric method, AGE, allometric growth equation. (b) Different independent variables. (c) Accuracy comparison between multi-source remote sensing and individual remote sensing data sources.

Table 4. Statistical table of sample with different independent variables.

| Independent variable | Number of samples | Sample proportion | <i>R</i> ² |
|----------------------|-------------------|-------------------|-----------------------|
| H | 14 | 18.42% | 98.4 |
| D | 10 | 13.16% | 77.4 |
| D ² H | 28 | 37.04% | 93.5 |
| Other | 24 | 31.58% | 95.3 |
| Total | 76 | 100% | |

Table 5. Statistical table of samples using different sensors.

| Sensor | Number of samples | Sample proportion | <i>R</i> ² |
|--------------|-------------------|-------------------|-----------------------|
| UAV lidar | 82 | 35.19% | 97.3 |
| Ground lidar | 52 | 22.32% | 75 |
| RGB | 40 | 17.17% | 93.5 |
| Spectra | 18 | 7.73% | 99.7 |
| Multi-source | 41 | 17.60% | 95.5 |
| Total | 233 | 100% | |

relatively sparse^[62,63]. The main reason for this result was that it could not overcome the problem of error accumulation in the process of single-tree estimation because of its limitation at the single-tree scale. This error not only exists in the calculation of single-tree AGB, but also in single-tree segmentation^[64]. Compared with the allometric growth equation, the non-parametric method has obvious advantages in estimating AGB on a large spatial scale. The non-parametric method could avoid the accumulated error in the estimations of single trees by using a small amount of plot data

as samples, and a more robust and accurate estimation model could be developed through continuous training, which could be applied to estimating the AGB of sample plots and large areas^[37,39]. These methods improved the estimation accuracy at the plot scale to a certain extent, but it was still significantly lower than that of ground lidar. Therefore, when estimating AGB at the single-tree and plot scales, ground lidar should be used as the preferred scheme. However, it should be noted that while ground lidar could provide detailed three-dimensional structural parameters of individual trees, without high-precision individual tree segmentation, accumulated errors from scale extrapolation (e.g., from single-tree to plot level) would significantly degrade the final accuracy.

In contrast, the performance of spectral methods at the stand scale remained suboptimal. This limitation primarily arose from the susceptibility of spectral data to atmospheric interference, such as cloud and fog cover, which significantly compromised the accuracy of data acquisition^[65,66]. Furthermore, the inherent complexity of the forest's vertical structure often resulted in the attenuation or loss of critical spectral signals^[67,68], thereby impeding optimal performance. As a consequence, the applicability of spectral approaches in large-scale, humid tropical rainforests was markedly constrained. Additionally, data saturation was a common issue in high-biomass environments^[69]. In regions characterized by dense vegetation cover or elevated leaf area index, the saturation of vegetation indices—particularly those relying on near-infrared reflectance—was especially pronounced^[68]. This saturation effect led to systematic underestimation of high biomass values, diminishing the overall accuracy of vegetation index-based AGB estimations. The

complexity of forest ecosystems further complicated the relationship between vegetation indices and biomass. For instance, in structurally heterogeneous environments, the correlation between the near-infrared band and biomass was substantially weaker compared with more homogeneous conditions^[70]. Moreover, many forest AGB models are based on stand-level structural variables, such as DBH and H^[71], parameters that are often unavailable in annually updated forest inventory datasets. This mismatch contributed to pronounced discrepancies between modeled estimates and ground truth observations. Collectively, these factors underscored the considerable limitations of relying solely on spectral methods for estimating forest AGB at the stand scale.

As the scale of research broadens, sensor selection must increasingly prioritize the comprehensiveness and representativeness of the acquired data to counteract the adverse effects of error accumulation on the accuracy of estimation. An expanding body of literature has underscored the value of integrating multi-source data across spatial scales and sensing platforms to enhance both the precision and reliability of forest AGB assessments. For example, ground lidar was frequently utilized to extract key structural parameters such as DBH and H, which were subsequently employed to construct AGB estimation models that are applicable to large-scale forested landscapes^[72,73]. This methodology is often complemented by auxiliary datasets—such as UAV lidar, hyperspectral, and multi-spectral imagery—for model support and validation of the accuracy. Such multi-source fusion not only significantly improves the precision of estimation but also effectively reduces the labor intensity and logistical complexity of large-scale data acquisition^[26,74].

Accuracy in different forest types

The complexity of forest types exerted a profound influence on the accuracy of AGB estimation, primarily through variations in spectral characteristics and canopy structure^[65,75]. Coniferous forests, characterized by their regular canopy architecture, were well-suited to the application of stereo registration algorithms in RGB imagery^[76,77]. In broadleaf forests, the biochemical and morphological uniformity of canopy foliage contributed to stable, linear relationships between spectral vegetation indices and AGB, facilitating accurate estimations^[47,78]. In contrast, mixed forests presented considerable structural complexity, with heterogeneous horizontal canopy arrangements and intricate vertical layering. These features induced multiple scattering of the spectral signals within the canopy, leading to signal saturation and a marked reduction in the accuracy of spectral estimation (ES = 0.66 in mixed forests, compared with ES = 0.84 in broadleaf forests and ES = 0.80 in coniferous forests). Furthermore, vegetation indices often failed to adequately suppress background interference^[79], particularly from exposed soil, thereby introducing additional noise and reducing the models' precision^[80].

Compared with models that relied exclusively on spectral data, integrated approaches that combined spectral information with structural data—such as lidar or photogrammetric metrics—consistently yielded higher accuracy in estimating forest AGB across diverse forest types^[10,56]. The findings highlighted the pronounced variation in estimation performance across both methodological approaches and forest types. At present, no universally applicable model exists for large-scale multi-species AGB estimation. Therefore, distinguishing forest types during model development is essential for enhancing the accuracy of estimation and ensuring robust application across heterogeneous forested landscapes^[81].

Accuracy with different research methods

The convergence in accuracy between ground-plot methods employing allometric equations and non-parametric approaches

underscored the scale-dependent nature of methodological selection. At the single-tree level, the reliability of allometric models was predominantly determined by the precision of input variables and the inherent robustness of the equations themselves; higher fidelity in these parameters directly enhanced the accuracy of AGB estimation^[50]. Measurement errors might arise from instrumental limitations, necessitating repeated sampling for correction, or from procedural inaccuracies. Moreover, AGB estimates derived through allometric models—whether targeting individual branches, foliage, or entire stands—were susceptible to the propagation of cumulative error, which can significantly distort AGB estimates at the plot or landscape scale. Such error transmission also occurred when DBH was inferred from H or vice versa^[82]. Increasing the sampling frequency and implementing standardized measurement protocols have proven effective in mitigating the propagation of error^[83,84]. It was also shown that model-related errors often stem from the geographically constrained applicability of allometric equations, which are typically region-specific and lack universal generalizability. Parametric methods, which established relationships between remote sensing-derived metrics and forest AGB, faced similar constraints in parameter accuracy, frequently caused by mismatches in spatial resolution or inconsistencies in measurement techniques^[82,85]. Regrettably, extracting robust predictive variables from raw datasets remains a challenge, particularly when data integrity is compromised by factors such as cloud cover disrupting the acquisition of the normalized differenced vegetation index or suboptimal atmospheric correction degrading the accuracy of surface reflectance.

Non-parametric approaches, supported by machine learning and deep learning techniques, offer a compelling solution to the limitations of parametric models by effectively capturing complex, non-linear relationships between remote sensing variables and AGB. Among these, deep learning exhibits considerable promise for estimating forest AGB, enabling the extraction of nuanced features related to vegetation density, species composition, and carbon storage, thus presenting a robust alternative to conventional regression-based frameworks. Nevertheless, the application of deep learning within close-range remote sensing contexts remains relatively underexplored and warrants greater scholarly attention. Recent studies in forestry have demonstrated the efficacy of deep learning models in predicting key structural parameters such as H and CW^[38,86].

Accordingly, future research should prioritize the adaptation and refinement of established deep learning architectures to better accommodate the heterogeneous conditions of forest ecosystems across different biogeographical regions and forest types^[87]. Advancements in this area will not only foster the integration of innovative computational methodologies in forest science but also provide critical technical support for the precise quantification of forest carbon stocks.

Accuracy with different independent variables

The results of the meta-analysis showed that D and D²H had the highest accuracy, and H had the lowest accuracy. The ES of D was slightly higher than that of D²H, indicating that its accuracy was more reliable. However, the accuracy of the D²H composite variable fluctuated less (95% CI: 0.81–0.93), indicating that it was more stable in most cases. The primary error associated with D²H stemmed from inaccuracy in estimating H. Although some studies have suggested that H is a powerful indicator for AGB estimation, accurate estimation of H has remained a significant challenge in forestry research, regardless of the method employed^[88]. Additionally, other studies have shown that incorporating H as an independent variable did not

significantly improve the model's accuracy^[29], and some scholars have strongly opposed including H as an independent variable in allometric growth equations^[89]. Instead, they favored using tree age or other variables, which also yielded satisfactory results. However, AGB equations using tree age as an independent variable were difficult to apply in natural forests, often leading to error propagation and greater uncertainty in estimates^[90], which, in turn, lowered the accuracy of AGB prediction models based on CW and H. These conclusions also explain why H was lower. In contrast, due to the mature DBH measurement technology, it remained stable in the field surveys, and the use of a model incorporating D would have higher accuracy. This indicated that the models using D are still the best choice in accessible areas.

Moreover, although increasing the number of independent variables would enhance the model fitting accuracy, it would also reduce the model's generalizability. Thus, when selecting independent variables, a balance must be struck between accuracy and generalizability to meet the requirements of various research scenarios. Therefore, selecting suitable independent variables for a study is critical, as an excessive focus on precision can be counter-productive. In practice, selecting easily measurable variables like DBH may better align with actual research needs^[28,91].

How to use multi-source remote sensing data to improve accuracy

With the continuous advancement of close-range remote sensing and forest AGB estimation research, multi-source data fusion has emerged as a critical strategy for enhancing estimation accuracy. By leveraging the complementary strengths of different sensors, multi-source fusion effectively addresses the inherent limitations of single-source data, thereby substantially improving the precision and robustness of AGB estimation. Depending on the stage of integration and the data acquisition platform, fusion strategies are generally categorized into data-level fusion and feature-level fusion^[11]. Data-level fusion involves the integration of raw data from different sensors or platforms prior to preprocessing. For example, ground-based and UAV-based point cloud datasets can be co-registered through spatial alignment techniques to create unified three-dimensional representations of forests^[92,93]. This form of fusion was particularly effective at the single-tree scale, where it was widely employed to enhance structural parameter retrieval and AGB estimation^[80]. Feature-level fusion, by contrast, entailed preprocessing data from multiple sources, extracting the relevant features, and then merging them into a composite dataset that synthesizes information across modalities. While spectral methods often struggle to capture key parameters for AGB estimation—such as H, DBH, and canopy metrics^[94,95]—lidar provides direct, high-precision measurements of these attributes, along with detailed representations of the forest's vertical and horizontal structure^[61,96]. Studies have consistently shown that integrating spectral and lidar data enhances estimation performance^[26]. Feature-level fusion could be further subdivided into point-based and object-based approaches. Point-based fusion was typically implemented at the plot and stand scales, wherein lidar point cloud data were rasterized onto a standardized grid and overlaid with multi-spectral or hyperspectral imagery^[97]. Object-based fusion, on the other hand, is more suited to the single-tree scale, involving the extraction of individual tree features and their subsequent integration across data sources. In addition, feature-level fusion could incorporate a wide range of auxiliary variables, including canopy closure, DEM, DTM, annual precipitation, mean annual temperature, and other non-vegetation factors such as climate conditions and soil fertility. The integration

of these variables further strengthen the reliability and accuracy of estimating forest AGB^[98–100].

Future research on multi-source remote sensing data should focus on the following three areas. The first is the development of new methods to process and fuse data from different sensors and platforms via multi-source, cross-scale, and cross-platform fusion, aiming to improve the accuracy of AGB estimation. This includes addressing issues of data scale diversity and scale transformation, optimizing cross-platform fusion technologies, ensuring data quality, and reducing uncertainties. Second, we should focus on the application of artificial intelligence, particularly deep learning, in analyzing complex relationships within forest ecosystems. Deep learning methods have shown immense potential, especially in predicting forest AGB^[37,39]. Future studies should explore the incorporation of cutting-edge deep learning algorithms from computer science into forest AGB estimations to meet AGB estimation needs across diverse regions and tree species. Lastly, there is significant variation among close-range remote sensing AGB estimation methods, and conclusions are often constrained by numerous factors. Therefore, determining the true values for verifying the accuracy remains a crucial issue. Harvesting methods have long been considered the most accurate and reliable, but in complex forest environments, ground-based field surveys are challenging and large-scale validation is not feasible. Currently, AGB estimation results based on close-range remote sensing techniques are primarily validated through plot sampling surveys or recent forest resource inventory data. These data are reported by provinces or regions, and due to varying levels of forestry development, there are considerable differences in accuracy and authenticity between the datasets.

Conclusions

This meta-analysis systematically evaluated close-range remote sensing techniques for AGB estimation, and addressed uncertainties arising from variations in the spatial scale, forest type, and methodological approach. The findings indicated that ground lidar consistently achieved the highest estimation accuracy across study scales, while UAV lidar demonstrated superior suitability for stand-scale assessments. Sensor performance varied substantially across forest types, emphasizing the necessity of incorporating different forest types when constructing models. The accuracy of the three primary methodological categories (parametric methods, non-parametric methods, and allometric growth equation models) was broadly comparable. However, the inclusion of composite variables such as DBH and H in allometric growth equation models notably enhanced the explanatory power. This study highlighted the inherent limitations of single-source data and demonstrated that multi-source data fusion effectively mitigates signal saturation and error accumulation from fine to broad spatial scales, particularly in structurally complex forests. By integrating complementary sensor capabilities, the fusion method has been shown to establish a robust paradigm for high-precision estimations of carbon stocks. Looking forward, the advancement of close-range remote sensing systems should focus on three key directions: (1) establishing standardized protocols for cross-platform integration of point cloud and spectral data; (2) developing multi-scale inversion models that synergize three-dimensional structural features with deep learning algorithms; and (3) constructing a non-destructive accuracy evaluation framework based on terrestrial laser scanning validation. Collectively, our research will provide critical scientific support for the precise quantification of forest carbon sinks in pursuit of carbon neutrality goals.

Author contributions

The authors confirm their contributions to the paper as follows: study conception and design: Liu J; data collection: Chen Z; analysis and interpretation of results: Liu J, Chen Z, Zhao Z; draft manuscript preparation: Liu J, Chen Z. All authors reviewed the results and approved the final version of the manuscript.

Data availability

All data underlying this study were systematically retrieved through a comprehensive meta-analysis of peer-reviewed literature (2010–2025). All data generated or analyzed during this study are included in this published article and its supplementary information files.

Acknowledgments

This study was sponsored by the National Natural Science Foundation of China (Grant Nos 32371875 and 32001249) and the Open Research Fund of the State Key Laboratory of Information Engineering in Surveying, Mapping and Remote Sensing, Wuhan University (Grant No. 24A01). We would like to acknowledge the partners who have contributed to this work. In addition, the authors would like to thank the anonymous reviewers for their helpful remarks.

Conflict of interest

The authors declare that they have no conflict of interest.

Supplementary information accompanies this paper at (<https://www.maxapress.com/article/doi/10.48130/forres-0025-0017>)

Dates

Received 17 March 2025; Revised 9 July 2025; Accepted 31 July 2025; Published online 21 August 2025

References

- Molotoks A, Stehfest E, Doelman J, Albanito F, Fitton N, et al. 2018. Global projections of future cropland expansion to 2050 and direct impacts on biodiversity and carbon storage. *Global Change Biology* 24:5895–908
- Tian L, Tao Y, Fu W, Li T, Ren F, et al. 2022. Dynamic simulation of land use/cover change and assessment of forest ecosystem carbon storage under climate change scenarios in Guangdong Province, China. *Remote Sensing* 14:2330
- Xiao J, Chevallier F, Gomez C, Guanter L, Hicke JA, et al. 2019. Remote sensing of the terrestrial carbon cycle: a review of advances over 50 years. *Remote Sensing of Environment* 233:111383
- Houghton RA, Hall F, Goetz SJ. 2009. Importance of biomass in the global carbon cycle. *Journal of Geophysical Research: Biogeosciences* 114:G00E03
- Pan Y, Birdsey RA, Fang J, Houghton R, Kauppi PE, et al. 2011. A large and persistent carbon sink in the world's forests. *Science* 333:988–93
- Zhao M, Yang J, Zhao N, Liu L, Du L, et al. 2021. Spatially explicit changes in forest biomass carbon of China over the past 4 decades: coupling long-term inventory and remote sensing data. *Journal of Cleaner Production* 316:128274
- Fang J, Kato T, Guo Z, Yang Y, Hu H, et al. 2014. Evidence for environmentally enhanced forest growth. *Proceedings of the National Academy of Sciences of the United States of America* 111:9527–32
- Lu D, Batistella M, Moran E. 2005. Satellite estimation of aboveground biomass and impacts of forest stand structure. *Photogrammetric Engineering and Remote Sensing* 71:967–74
- Avitabile V, Camia A. 2018. An assessment of forest biomass maps in Europe using harmonized national statistics and inventory plots. *Forest Ecology and Management* 409:489–98
- Du Y, Wang J, Liu Z, Yu H, Li Z, et al. 2019. Evaluation on spaceborne multispectral images, airborne hyperspectral, and lidar data for extracting spatial distribution and estimating aboveground biomass of wetland vegetation *Suaeda salsa*. *IEEE Journal of Selected Topics in Applied Earth Observations and Remote Sensing* 12:200–9
- Balestra M, Marselis S, Sankey TT, Cabo C, Liang X, et al. 2024. lidar data fusion to improve forest attribute estimates: a review. *Current Forestry Reports* 10:281–97
- Yan R, Dong Y, Li Y, Xu C, Luan Q, et al. 2024. Enhancing genomic association studies in slash pine through close-range UAV-based morphological phenotyping. *Forestry Research* 4:e025
- Bazrafkan A, Delavarpour N, Oduor PG, Bandillo N, Flores P. 2023. An overview of using unmanned aerial system mounted sensors to measure plant above-ground biomass. *Remote Sensing* 15:3543
- da Silva BRF, Ucella-Filho JGM, da Conceição Bispo P, Elera-Gonzales DG, Silva EA, et al. 2024. Using drones for dendrometric estimations in forests: a bibliometric analysis. *Forests* 15:1993
- Liu J, Feng Z, Mannan A, Yang L. 2019. Positioning of coordinates and precision analysis of sample trees using the intelligent forest survey calculator. *Computers and Electronics in Agriculture* 159:157–64
- Liu J, Feng Z, Yang L, Mannan A, Khan TU, et al. 2018. Extraction of sample plot parameters from 3D point cloud reconstruction based on combined RTK and CCD continuous photography. *Remote Sensing* 10:1299
- Santoro M, Beaudoin A, Beer C, Cartus O, Franssón JES, et al. 2015. Forest growing stock volume of the Northern Hemisphere: spatially explicit estimates for 2010 derived from Envisat ASAR. *Remote Sensing of Environment* 168:316–34
- Badreldin N, Sanchez-Azofeifa A. 2015. Estimating forest biomass dynamics by integrating multi-temporal landsat satellite images with ground and airborne lidar data in the coal valley mine, Alberta, Canada. *Remote Sensing* 7:2832–49
- Kim Y, Chang A, Kim Y, Song J, Kim C. 2012. Estimation of forest biomass from airborne lidar data as measures against global warming-individual tree unit and forest stand unit. *Disaster Advances* 5:295–99
- Torre-Tojal L, Bastarrika A, Boyano A, Manuel Lopez-Guede JM, Graña M. 2022. Above-ground biomass estimation from lidar data using random forest algorithms. *Journal of Computational Science* 58:101517
- Yu Q, Yue C, Luo H, Luo F, Duan Y, et al. 2024. Forest AGB estimation based on airborne L-band full-polarization UAVSAR. *Forest Engineering* 40:17–29 (In Chinese)
- Zhang T, Chen S, Cao S. 2025. Building and application of an estimation method for urban forest aboveground biomass based on UAV lidar and optical images. *Journal of Nanjing University of Information Science & Technology* 17:581–90 (In Chinese)
- Liang X, Kankare V, Hyypää J, Wang Y, Kukko A, et al. 2016. Terrestrial laser scanning in forest inventories. *ISPRS Journal of Photogrammetry and Remote Sensing* 115:63–77
- Vauhkonen J, Korpela I, Maltamo M, Tokola T. 2010. Imputation of single-tree attributes using airborne laser scanning-based height, intensity, and alpha shape metrics. *Remote Sensing of Environment* 114:1263–76
- Hauglin M, Gobakken T, Astrup R, Ene L, Næsset E. 2014. Estimating single-tree crown biomass of Norway spruce by airborne laser scanning: a comparison of methods with and without the use of terrestrial laser scanning to obtain the ground reference data. *Forests* 5:384–403
- Lefsky MA, Cohen WB, Harding DJ, Parker GG, Acker SA, et al. 2002. Lidar remote sensing of above-ground biomass in three biomes. *Global Ecology and Biogeography* 11:393–99
- Messinger M, Asner GP, Silman M. 2016. Rapid assessments of Amazon forest structure and biomass using small unmanned aerial systems. *Remote Sensing* 8:615
- Wu H, Xu H. 2023. A review of sampling and modeling techniques for forest biomass inventory. *Agricultural & Rural Studies* 1:2
- Basuki TM, van Laake PE, Skidmore AK, Hussin YA. 2009. Allometric equations for estimating the above-ground biomass in tropical lowland Dipterocarp forests. *Forest Ecology and Management* 257:1684–94

30. Nelson R, Oderwald R, Gregoire TG. 1997. Separating the ground and airborne laser sampling phases to estimate tropical forest basal area, volume, and biomass. *Remote Sensing of Environment* 60:311–26
31. Almeida A, Gonçalves F, Silva G, Souza R, Treuhaft R, et al. 2020. Estimating structure and biomass of a secondary Atlantic forest in Brazil using Fourier transforms of vertical profiles derived from UAV photogrammetry point clouds. *Remote Sensing* 12:3560
32. Bendig J, Bolten A, Bennertz S, Broscheit J, Eichfuss S, et al. 2014. Estimating biomass of barley using crop surface models (CSMs) derived from UAV-based RGB imaging. *Remote Sensing* 6:10395–412
33. Wang X, Wang S, Dai L. 2018. Estimating and mapping forest biomass in Northeast China using joint forest resources inventory and remote sensing data. *Journal of Forestry Research* 29:797–811
34. Zhang D, Ni H. 2023. Inversion of forest biomass based on multi-source remote sensing images. *Sensors* 23:9313
35. Oehmcke S, Li L, Trepekli K, Revenga JC, Nord-Larsen T, et al. 2024. Deep point cloud regression for above-ground forest biomass estimation from airborne lidar. *Remote Sensing of Environment* 302:113968
36. Liu H, Mou C, Yuan J, Chen Z, Zhong L, et al. 2024. Estimating urban forests biomass with lidar by using deep learning foundation models. *Remote Sensing* 16:1643
37. Huy B, Truong NQ, Khiem NQ, Poudel KP, Temesgen H. 2022. Deep learning models for improved reliability of tree aboveground biomass prediction in the tropical evergreen broadleaf forests. *Forest Ecology and Management* 508:120031
38. Choi K, Lim W, Chang B, Jeong J, Kim I, et al. 2022. An automatic approach for tree species detection and profile estimation of urban street trees using deep learning and Google street view images. *ISPRS Journal of Photogrammetry and Remote Sensing* 190:165–80
39. Huy B, Truong NQ, Poudel KP, Temesgen H, Khiem NQ. 2024. Multi-output deep learning models for enhanced reliability of simultaneous tree above- and below-ground biomass predictions in tropical forests of Vietnam. *Computers and Electronics in Agriculture* 222:109080
40. Tian X, Li J, Zhang F, Zhang H, Jiang M. 2024. Forest aboveground biomass estimation using multisource remote sensing data and deep learning algorithms: a case study over Hangzhou area in China. *Remote Sensing* 16:1074
41. Central People's Government of the People's Republic of China. 2021. *The fifth plenary session of the 19th CPC Central Committee held in Beijing from October 26 to 29 adopted the Party leadership's proposals for formulating the 14th Five-Year Plan (2021–2025) for National Economic and Social Development and the Long-Range Objectives Through the Year 2035*
42. Zhang R, Zhou X, Ouyang Z, Avitabile V, Qi J, et al. 2019. Estimating aboveground biomass in subtropical forests of China by integrating multisource remote sensing and ground data. *Remote Sensing of Environment* 232:111341
43. Luo Y, Hui D, Zhang D. 2006. Elevated CO₂ stimulates net accumulations of carbon and nitrogen in land ecosystems: a meta-analysis. *Ecology* 87:53–63
44. Zhang Z, Zhu L. 2023. A review on unmanned aerial vehicle remote sensing: platforms, sensors, data processing methods, and applications. *Drones* 7:398
45. Brede B, Terry L, Barbier N, Bartholomeus HM, Bartolo R, et al. 2022. Non-destructive estimation of individual tree biomass: allometric models, terrestrial and UAV laser scanning. *Remote Sensing of Environment* 280:113180
46. Tao Z, Yi L, Bao A, Xu W, Wang Z, et al. 2024. UAV or satellites? How to find the balance between efficiency and accuracy in above ground biomass estimation of artificial young coniferous forest? *International Journal of Applied Earth Observation and Geoinformation* 134:104173
47. Ferreira MP, Martins GB, de Almeida TMH, da Silva Ribeiro R, da Veiga VF Jr, et al. 2024. Estimating aboveground biomass of tropical urban forests with UAV-borne hyperspectral and lidar data. *Urban Forestry & Urban Greening* 96:128362
48. Huang W, Dolan K, Swatantran A, Johnson K, Tang H, et al. 2019. High-resolution mapping of aboveground biomass for forest carbon monitoring system in the Tri-State region of Maryland, Pennsylvania and Delaware, USA. *Environmental Research Letters* 14:095002
49. Zurqani HA. 2025. A multi-source approach combining GEDI lidar, satellite data, and machine learning algorithms for estimating forest aboveground biomass on Google Earth Engine platform. *Ecological Informatics* 86:103052
50. Liu X, Dong L, Li S, Li Z, Wang Y, et al. 2024. Improving AGB estimations by integrating tree height and crown radius from multisource remote sensing. *PLoS One* 19:e0311642
51. Chen Q, McRoberts RE, Wang C, Radtke PJ. 2016. Forest aboveground biomass mapping and estimation across multiple spatial scales using model-based inference. *Remote Sensing of Environment* 184:350–60
52. Stovall AEL, Vorster AG, Anderson RS, Evangelista PH, Shugart HH. 2017. Non-destructive aboveground biomass estimation of coniferous trees using terrestrial lidar. *Remote Sensing of Environment* 200:31–42
53. Liang X, Kukko A, Balenović I, Saarinen N, Junttila S, et al. 2022. Close-range remote sensing of forests: the state of the art, challenges, and opportunities for systems and data acquisitions. *IEEE Geoscience and Remote Sensing Magazine* 10:32–71
54. Wang D, Momo Takoudjou S, Casella E. 2020. LeWoS: a universal leaf-wood classification method to facilitate the 3D modelling of large tropical trees using terrestrial lidar. *Methods in Ecology and Evolution* 11:376–89
55. Gómez-Díaz JD, Etchevers-Barra JD, Monterrosos-Rivas AI, Campo-Alvez J, Tinoco-Rueda JA. 2011. Allometric equations for estimating the above-ground biomass and carbon in *Quercus magnoliaefolia* Née. *Revista Chapingo Serie Ciencias Forestales y del Ambiente* 17:261–72
56. Hemming-Schroeder NM, Gutierrez AA, Allison SD, Randerson JT. 2023. Estimating individual tree mortality in the Sierra Nevada using lidar and multispectral reflectance data. *Journal of Geophysical Research: Biogeosciences* 128:e2022JG007234
57. Maltamo M, Eerikainen K, Pitkanen J, Hyypä J, Vehmas M. 2004. Estimation of timber volume and stem density based on scanning laser altimetry and expected tree size distribution functions. *Remote Sensing of Environment* 90:319–30
58. Næsset E. 1997. Determination of mean tree height of forest stands using airborne laser scanner data. *ISPRS Journal of Photogrammetry and Remote Sensing* 52:49–56
59. Apostol B, Lorent A, Petrila M, Gancz V, Badea O. 2016. Height extraction and stand volume estimation based on fusion airborne lidar data and terrestrial measurements for a norway spruce [*Picea abies* (L.) Karst.] test site in Romania. *Notulae Botanicae Horti Agrobotanici Cluj-Napoca* 44:313–23
60. Qin H, Zhou W, Yao Y, Wang W. 2021. Estimating aboveground carbon stock at the scale of individual trees in subtropical forests using UAV lidar and hyperspectral data. *Remote Sensing* 13:4969
61. Tang H, Ma L, Lister A, O'Neill-Dunne J, Lu J, et al. 2021. High-resolution forest carbon mapping for climate mitigation baselines over the RGGI region, USA. *Environmental Research Letters* 16:035011
62. Ene LT, Næsset E, Gobakken T, Bollandsås OM, Maurya EW, et al. 2017. Large-scale estimation of change in aboveground biomass in miombo woodlands using airborne laser scanning and national forest inventory data. *Remote Sensing of Environment* 188:106–17
63. Hansen EH, Gobakken T, Solberg S, Kangas A, Ene L, et al. 2015. Relative efficiency of ALS and InSAR for biomass estimation in a Tanzanian rainforest. *Remote Sensing* 7:9865–85
64. Qin H, Zhou W, Yao Y, Wang W. 2022. Individual tree segmentation and tree species classification in subtropical broadleaf forests using UAV-based lidar, hyperspectral, and ultrahigh-resolution RGB data. *Remote Sensing of Environment* 280:113143
65. Cho MA, Skidmore A, Corsi F, van Wieren SE, Sobhan I. 2007. Estimation of green grass/herb biomass from airborne hyperspectral imagery using spectral indices and partial least squares regression. *International Journal of Applied Earth Observation and Geoinformation* 9:414–24
66. Jiang R, Sanchez-Azofeifa A, Laakso K, Xu Y, Zhou Z, et al. 2021. Cloud cover throughout all the paddy rice fields in Guangdong, China: impacts on sentinel 2 MSI and landsat 8 OLI optical observations. *Remote Sensing* 13:2961
67. Yang T, Yu Y, Yang X, Du H. 2023. UAV hyperspectral combined with lidar to estimate chlorophyll content at the stand and individual tree scales. *Chinese Journal of Applied Ecology* 34:2101–12

68. Mutanga O, Skidmore AK. 2004. Narrow band vegetation indices overcome the saturation problem in biomass estimation. *International Journal of Remote Sensing* 25:3999–4014
69. Puliti S, Hauglin M, Breidenbach J, Montesano P, Neigh CSR, et al. 2020. Modelling above-ground biomass stock over Norway using national forest inventory data with ArcticDEM and Sentinel-2 data. *Remote Sensing of Environment* 236:111501
70. Hao Q, Huang C. 2023. A review of forest aboveground biomass estimation based on remote sensing data. *Journal of Plant Ecology* 47:1356–74
71. Zou W, Zeng W. 2025. Research Advances in Estimation of Forest Biomass and Carbon Storage. *World Forestry Research* 38:32–38 (In Chinese)
72. Hauglin M, Astrup R, Gobakken T, Næsset E. 2013. Estimating single-tree branch biomass of Norway spruce with terrestrial laser scanning using voxel-based and crown dimension features. *Scandinavian Journal of Forest Research* 28:456–69
73. Du L, Zhou T, Zou Z, Zhao X, Huang K, et al. 2014. Mapping forest biomass using remote sensing and national forest inventory in China. *Forests* 5:1267–83
74. Beyene SM. 2020. Estimation of forest variable and aboveground biomass using Terrestrial laser scanning in the tropical rainforest. *Journal of the Indian Society of Remote Sensing* 48:853–63
75. Bargali K, Manral V, Padalia K, Bargali SS, Upadhyay VP. 2018. Effect of vegetation type and season on microbial biomass carbon in central himalayan forest soils, India. *CATENA* 171:125–35
76. Liu J, Guo Y, Yang J, Zhu N, Dai W, et al. 2024. Forest point cloud registration: a review. *Forestry Research* 4:e018
77. Liu J, Guo Y, Zeng J, Chen Z, Wang H, et al. 2024. Forest point cloud registration using the tree top and the ground-level tree center. *Transactions of the Chinese Society of Agricultural Engineering* 40:127–34 (In Chinese)
78. Yan M, Xia Y, Yang X, Wu X, Yang M, et al. 2023. Biomass estimation of subtropical arboreal forest at single tree scale based on feature fusion of airborne lidar data and aerial images. *Sustainability* 15:1676
79. Ahmed S, Hilmers T, Uhl E, Tupinambá-Simões F, Ordóñez C, et al. 2025. From suppressed to dominant: 3D crown shapes explain the "to grow or wait" growth behavior in close-to-nature forests. *Forest Ecology and Management* 592:122814
80. Li J, Zhang W, Diao W, Feng Y, Sun X, et al. 2022. CSF-net: color spectrum fusion network for semantic labeling of airborne laser scanning point cloud. *IEEE Journal of Selected Topics in Applied Earth Observations and Remote Sensing* 15:339–52
81. Pang Y, Zhao F, Li Z, Zhou S, Deng G, et al. 2008. Forest height inversion using airborne lidar technology. *Journal of Remote Sensing* 12:152–58 (In Chinese)
82. Mascaro J, Detto M, Asner GP, Muller-Landau HC. 2011. Evaluating uncertainty in mapping forest carbon with airborne lidar. *Remote Sensing of Environment* 115:3770–74
83. Breidenbach J, Antón-Fernández C, Petersson H, McRoberts RE, Astrup R. 2014. Quantifying the model-related variability of biomass stock and change estimates in the Norwegian national forest inventory. *Forest Science* 60:25–33
84. Gao BC, Li RR. 2000. Quantitative improvement in the estimates of NDVI values from remotely sensed data by correcting thin cirrus scattering effects. *Remote Sensing of Environment* 74:494–502
85. Keller M, Palace M, Hurr G. 2001. Biomass estimation in the Tapajos National Forest, Brazil: examination of sampling and allometric uncertainties. *Forest Ecology and Management* 154:371–82
86. Ercanlı İ. 2020. Innovative deep learning artificial intelligence applications for predicting relationships between individual tree height and diameter at breast height. *Forest Ecosystems* 7:12
87. Fararoda R, Reddy RS, Rajashekar G, Kiran Chand TR, Jha CS, et al. 2021. Improving forest above ground biomass estimates over indian forests using multi source data sets with machine learning algorithm. *Ecological Informatics* 65:101392
88. Peng X, Zhao A, Chen Y, Chen Q, Liu H. 2021. Tree height measurements in degraded tropical forests based on UAV-lidar data of different point cloud densities: a case study on *Dacrydium pierrei* in China. *Forests* 12:328
89. Leuschner C, Moser G, Bertsch C, Röderstein M, Hertel D. 2007. Large altitudinal increase in tree root/shoot ratio in tropical mountain forests of Ecuador. *Basic and Applied Ecology* 8:219–30
90. Maltamo M, Kinnunen H, Kangas A, Korhonen L. 2020. Predicting stand age in managed forests using national forest inventory field data and airborne laser scanning. *Forest Ecosystems* 7:44
91. Wu J, Zhu J, Ai X, Yao L, Guo Q, et al. 2023. Meta-analysis of woody plant biomass models in subtropical evergreen and deciduous broad-leaved mixed forests. *Journal of Central South University of Forestry and Technology* 43:111–22 (In Chinese)
92. Dai W, Kan H, Tan R, Yang B, Guan Q, et al. 2022. Multisource forest point cloud registration with semantic-guided keypoints and robust RANSAC mechanisms. *International Journal of Applied Earth Observation and Geoinformation* 115:103105
93. Wang Y, Zhao J, Guo Z, Yang H, Li N. 2023. Soil moisture inversion based on data augmentation method using multi-source remote sensing data. *Remote Sensing* 15:1899
94. Tian L, Wu X, Tao Y, Li M, Qian C, et al. 2023. Review of remote sensing-based methods for forest aboveground biomass estimation: progress, challenges, and prospects. *Forests* 14:1086
95. Fang J, Brown S, Tang Y, Nabuurs GJ, Wang X, et al. 2006. Overestimated biomass carbon pools of the northern mid- and high latitude forests. *Climatic Change* 74:355–68
96. Zhu Y, Feng Z, Lu J, Liu J. 2020. Estimation of forest biomass in Beijing (China) using multisource remote sensing and forest inventory data. *Forests* 11:163
97. Clark ML, Clark DB, Roberts DA. 2004. Small-footprint lidar estimation of sub-canopy elevation and tree height in a tropical rain forest landscape. *Remote Sensing of Environment* 91:68–89
98. Hall RJ, Skakun RS, Arsenault EJ, Case BS. 2006. Modeling forest stand structure attributes using Landsat ETM+ data: application to mapping of aboveground biomass and stand volume. *Forest Ecology and Management* 225:378–90
99. Main-Knorn M, Moisen GG, Healey SP, Keeton WS, Freeman EA, et al. 2011. Evaluating the remote sensing and inventory-based estimation of biomass in the western carpathians. *Remote Sensing* 3:1427–46
100. Zhuang H, Zhang Z, Cheng F, Han J, Luo Y, et al. 2024. Integrating data assimilation, crop model, and machine learning for winter wheat yield forecasting in the North China Plain. *Agricultural and Forest Meteorology* 347:109909



Copyright: © 2025 by the author(s). Published by Maximum Academic Press, Fayetteville, GA. This article is an open access article distributed under Creative Commons Attribution License (CC BY 4.0), visit <https://creativecommons.org/licenses/by/4.0/>.